

Fractionalized Charge Excitations in a Spin Liquid on Partially Filled Pyrochlore Lattices

Gang Chen,¹ Hae-Young Kee,^{1,3} and Yong Baek Kim^{1,2,3}

¹*Department of Physics, University of Toronto, Toronto, Ontario M5S1A7, Canada*

²*School of Physics, Korea Institute for Advanced Study, Seoul 130-722, Korea*

³*Canadian Institute for Advanced Research/Quantum Materials Program, Toronto, Ontario MSG 1Z8, Canada*

(Received 26 March 2014; published 7 November 2014; publisher error corrected 10 November 2014)

We study the Mott transition from a metal to cluster Mott insulators in the 1/4- and 1/8-filled pyrochlore lattice systems. It is shown that such Mott transitions can arise due to charge localization in clusters or in tetrahedron units, driven by the nearest-neighbor repulsive interaction. The resulting cluster Mott insulator is a quantum spin liquid with a spinon Fermi surface, but at the same time a novel fractionalized charge liquid with charge excitations carrying half the electron charge. There exist two emergent U(1) gauge fields or “photons” that mediate interactions between spinons and charge excitations, and between fractionalized charge excitations themselves, respectively. In particular, it is suggested that the emergent photons associated with the fractionalized charge excitations can be measured in x-ray scattering experiments. Various other experimental signatures of the exotic cluster Mott insulator are discussed in light of candidate materials with partially filled bands on the pyrochlore lattice.

DOI: 10.1103/PhysRevLett.113.197202

PACS numbers: 75.10.Kt, 05.30.Rt

In Mott insulators, strong correlation causes the charge localization [1]. As the charge excitation gap becomes smaller near the insulator-metal transition, the strong local charge fluctuations can generate significant long-range and/or ring exchange spin interactions. It has been recognized that these interactions may stabilize the so-called quantum spin liquid (QSL) [2,3], where there exist charge-neutral spin-1/2 excitations or spinons while spinless charge excitations are gapped [4]. In particular, when the transition from a metal to the spin liquid is continuous, the resulting spin liquid may form a Fermi surface of the spinons. In the study of a Hubbard model at the $\frac{1}{2}$ filling for the 2D triangular and 3D hyperkagome lattices [5–7], this new type of Mott transition is shown to occur as one increases the on-site Hubbard interaction. On the experimental front, such transitions can be of relevance to QSL candidate materials such as the 2D triangular lattice organic compound κ -(ET)₂Cu₂(CN)₃ [8] and the 3D hyperkagome material Na₄Ir₃O₈ [9]. In this spin liquid state, the spinons are interacting with an emergent U(1) gauge field or “photon”; hence, it is called the U(1) QSL [2,3,5–7,10]. On the other hand, the charge excitations behave trivially and are simply localized on the lattice sites forming a charge “solid” with gapped charge q_e excitations. One may wonder whether it is possible to have a Mott insulator where the charge physics becomes nontrivial in addition to the spin sector.

In this Letter, we study Mott insulators and Mott transitions in partially filled pyrochlore lattice systems. We uncover a novel cluster Mott insulator (CMI), where the electrons are localized within the tetrahedral clusters rather than on lattice sites. An example of a CMI on the kagome lattice has recently been discovered in LiZn₂Mo₃O₈ and

studied by us theoretically [11,12]. The ground state of the CMI on the pyrochlore lattice is shown to be a quantum spin liquid where there exist fractionalized charge excitations in addition to gapped spinons, and two kinds of emergent gauge photons. Although the notion of charge fractionalization has been proposed in certain classically degenerate systems [13], the charge fractionalization discussed in this Letter is fundamentally different and is an intrinsic quantum effect. Besides the fundamental interest, this problem is of interest from the experimental point of view. Pyrochlore lattice systems with partially filled bands occur in various materials with mixed-valence magnetic ions [14–17]. The model and underlying physics discussed in our work would potentially be relevant to such systems.

We focus on a single-band Hubbard model,

$$H = -t \sum_{\langle ij \rangle, \sigma} (c_{i\sigma}^\dagger c_{j\sigma} + \text{H.c.}) - \mu \sum_i n_i + V \sum_{\langle ij \rangle} n_i n_j + \frac{U}{2} \sum_i \left(n_i - \frac{1}{2} \right)^2, \quad (1)$$

where $c_{i\sigma}^\dagger$ ($c_{i\sigma}$) is the electron creation (annihilation) operator at site i with spin σ and n_i ($n_i = \sum_\sigma n_{i\sigma}$) is the electron number operator. We consider $\frac{1}{4}$ - and $\frac{1}{8}$ -filled cases. Throughout this Letter, we assume that the on-site Hubbard U is the biggest energy scale. Notice, however, that the interaction U cannot cause electron localization for a partially filled band. It is the nearest-neighbor repulsion V that drives the charge localization and the formation of Mott insulators. Similarly to the $\frac{1}{2}$ -filled case, the spin sector may form a QSL with a spinon Fermi surface for

sufficiently large V . In contrast to the $\frac{1}{2}$ -filled case, however, the electrons in the Mott regime are localized on tetrahedral clusters with two (one) electrons per tetrahedron in the $\frac{1}{4}$ ($\frac{1}{8}$)-filled case. In the classical $V = \infty$ limit, the electron site-occupation configurations of this CMI are highly degenerate [18]. This is analogous to the degenerate ground-state manifold in the classical spin ice [19] ($\frac{1}{2}$ -magnetization plateau state [20]) for the $\frac{1}{4}$ ($\frac{1}{8}$)-filled case.

It is shown that, at finite V , the charge sector supports an additional emergent U(1) gauge field and fractionalization of charge quantum number in analogy to the quantum spin ice or $\frac{1}{2}$ -magnetization plateau state. Therefore, the charge sector of the CMI is a U(1) fractionalized charge liquid (FCL). We show that the electron in this CMI fractionalizes into a fermionic spinon and two charge bosons that carry *half the electron charge*. The transition to a Fermi liquid metal occurs when the fractionally-charged bosons condense. We also discuss thermodynamic and spectroscopic properties of this novel Mott insulating phase.

Weak Mott regime for $\frac{1}{4}$ filling. We start with the $\frac{1}{4}$ filled case. The model has a Fermi liquid ground state for $V \ll t$ [21] and a Mott insulating ground state for $V \gg t$. To study the Mott transition of this Hubbard model, we first introduce the usual slave rotor formalism [3,22] and express the electron operator as $c_{i\sigma}^\dagger = e^{i\theta_i} f_{i\sigma}^\dagger$, where $e^{i\theta_i}$ is the bosonic rotor operator carrying electric charge q_e and $f_{i\sigma}^\dagger$ is the charge-neutral fermionic spinon operator. To preserve the physical Hilbert space, we impose the gauge constraint $L_i^z = (\sum_{\sigma} f_{i\sigma}^\dagger f_{i\sigma}) - \frac{1}{2}$, where L_i^z is the conjugate operator of θ_j with $[\theta_i, L_j^z] = i\delta_{ij}$. Via a decoupling of the electron hopping term, the original Hubbard model is reduced to two coupled Hamiltonian H_{sp} and H_{ch} for the spin and charge sectors, respectively,

$$H_{\text{sp}} = -\sum_{\langle ij \rangle, \sigma} t_{ij}^{\text{eff}} (f_{i\sigma}^\dagger f_{j\sigma} + \text{H.c.}) - \sum_{i, \sigma} (\mu + h_i) f_{i\sigma}^\dagger f_{i\sigma} \quad (2)$$

$$H_{\text{ch}} = -\sum_{\langle ij \rangle} J_{ij}^{\text{eff}} (e^{i\theta_i - i\theta_j} + \text{H.c.}) + V \sum_{\langle ij \rangle} L_i^z L_j^z + 3V \sum_i L_i^z + \sum_i h_i \left(L_i^z + \frac{1}{2} \right) + \frac{U}{2} \sum_i (L_i^z)^2. \quad (3)$$

Here, $t_{ij}^{\text{eff}} = t \langle e^{i\theta_i - i\theta_j} \rangle \equiv |t_{ij}^{\text{eff}}| e^{ia_{ij}}$, $J_{ij}^{\text{eff}} = t \sum_{\sigma} \langle f_{i\sigma}^\dagger f_{j\sigma} \rangle \equiv |J_{ij}^{\text{eff}}| e^{-ia_{ij}}$ and h_i is the Lagrange multiplier that imposes the Hilbert space constraint. With this reformulation of the Hubbard model, the Hamiltonians H_{sp} and H_{ch} are now invariant under an internal U(1) gauge transformation $f_{i\sigma}^\dagger \rightarrow f_{i\sigma}^\dagger e^{-i\chi_i}$, $\theta_i \rightarrow \theta_i + \chi_i$ and $a_{ij} \rightarrow a_{ij} + \chi_i - \chi_j$. This internal U(1) gauge structure will be referred as U(1)_{sp} in the following.

In the $\frac{1}{2}$ filled case, the electrons are localized on the lattice sites in the Mott insulator. In the slave rotor

formulation, the QSL Mott insulator corresponds to the deconfined phase of the U(1)_{sp} gauge theory, and its transition to the metallic phase is induced by the condensation of the charge rotor [3,22]. The situation for $\frac{1}{4}$ filling is somewhat different, even though the spin sector behaves similarly and forms a U(1)_{sp} QSL with a spinon Fermi surface in the Mott regime. For the charge sector, the strong inter-site repulsion $(V/2) \sum_{\text{tet}} (\sum_{i \in \text{tet}} L_i^z)^2 + \text{const}$ (where tet refers to a tetrahedron) penalizes single charge motion from one tetrahedral cluster to another and leads to charge localization on the cluster. Hence, the total charge number on each tetrahedra is constrained to be two, or equivalently, satisfies the *charge ice constraint* $\sum_{i \in \text{tet}} L_i^z = 0$, which is reminiscent of the spin ice constraint in the classical spin ice [19,23–27]. Similarly to the classical spin ice [19], the classical charge ice configurations in the infinite V limit are macroscopically degenerate [13,18]. These features drastically modify the charge sector physics.

We now adopt a self-consistent mean-field approach and assume a uniform slave-rotor mean-field solution such that $t_{ij}^{\text{eff}} \equiv t^{\text{eff}}$, $J_{ij}^{\text{eff}} \equiv J^{\text{eff}}$, and $h_i \equiv h$. In the CMI, the rotor hopping J^{eff} introduces quantum fluctuations and lifts the extensive charge ice degeneracy, which is captured by a standard perturbative treatment of J^{eff} . We preserve the charge ice constraint in the ground state and obtain an effective ring rotor hopping model from the third-order degenerate perturbation theory,

$$H_{\text{ch,eff}} = -J_{\text{ring}} \sum_{\text{hexagon}} \cos(\theta_1 - \theta_2 + \theta_3 - \theta_4 + \theta_5 - \theta_6) + \frac{U}{2} \sum_i (L_i^z)^2, \quad (4)$$

where $J_{\text{ring}} = 24(J^{\text{eff}})^3/V^2$ is the ring rotor-hopping amplitude around a hexagon plaquette [see Fig. 1(a)]. This low-energy effective model acts on the charge ice manifold and is analogous to the one obtained in the context of the quantum spin ice in the XXZ model [26] on the pyrochlore lattice except that we have a large and finite interaction U and L^z can take the values of $\pm \frac{1}{2}$ and $\frac{3}{2}$ at the lattice length scale. Despite these small differences, the current model does share the same internal symmetries as the quantum spin ice models and thus the universal properties of our model $H_{\text{ch,eff}}$ is identical to the quantum spin ice in the low energy limit with $L^z = \pm \frac{1}{2}$. Therefore, the ground state of the charge sector is a U(1) *quantum charge ice*. The low energy U(1) gauge structure is obtained by introducing lattice electric field $L_i^z \sim E_{\mathbf{r}\mathbf{r}'}$ and lattice vector potential $e^{i\theta_i} \sim e^{iA_{\mathbf{r}'}}$, where $\mathbf{r}(\mathbf{r}')$ lies on the A(B) diamond sublattice [Fig. 1(c)] and $E_{\mathbf{r}\mathbf{r}'} = -E_{\mathbf{r}'\mathbf{r}}$, $A_{\mathbf{r}\mathbf{r}'} = -A_{\mathbf{r}'\mathbf{r}}$. To distinguish it from the U(1)_{sp} gauge field, we label this as U(1)_{ch} gauge field for the charge sector. The CMI is in the deconfined phase of this compact U(1)_{ch} gauge theory and we expect a

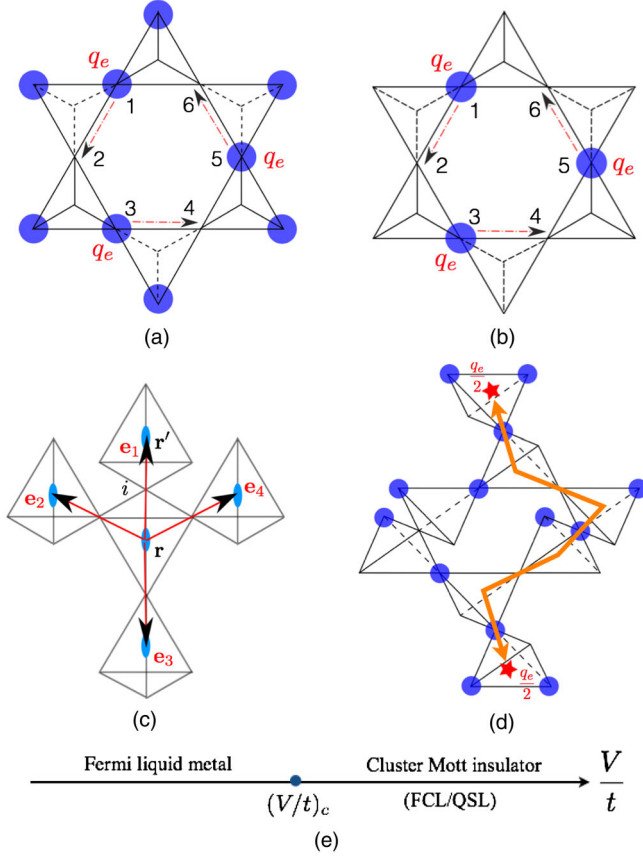


FIG. 1 (color online). The ring hopping processes of charge rotors around a hexagon in the CMI, for the $\frac{1}{4}$ and $\frac{1}{8}$ -filled cases shown in (a) and (b). As shown in (c), \mathbf{r} and \mathbf{r}' are located on the center of the tetrahedra and form a dual diamond lattice. We use \mathbf{r}, \mathbf{r}' (i, j) to label the diamond (pyrochlore) lattice sites. In (c), $\mathbf{r} \in A$ diamond sublattice and \mathbf{e}_μ are four vectors connecting A sublattice sites to the four neighboring B sublattice sites. In (d), the electron charge fractionalization in the FCL/QSL phase is illustrated. The two end charge defects are connected by a fictitious string. The phase diagram at the $\frac{1}{4}$ or $\frac{1}{8}$ -filling is plotted in (e). Here, $(V/t)_c = 1.65(0.98)$ for the $\frac{1}{4}$ ($\frac{1}{8}$)-filling in the mean-field theory. There are only two phases: a Fermi liquid metal and a CMI (FCL/QSL).

gapless and linearly dispersing $U(1)_{\text{ch}}$ gauge photon to appear at low energies.

Beyond the low energy regime, the rotor operator $e^{i\theta_i}$ creates a gapped charge- q_e excitation that violates the charge ice constraints on the two neighboring tetrahedra centered at \mathbf{r} and \mathbf{r}' . Just like the spin- $\frac{1}{2}$ bosonic spinon excitations in quantum spin ice, this defect charge- q_e excitation can be separated into two deconfined charge bosons (Φ^\dagger) in arbitrary distances, each carrying half the electron charge. Therefore, the quantum charge ice state is a $U(1)$ fractionalized charge liquid (FCL). As shown in Table I, these two fractionally charged bosons also carry the $U(1)_{\text{sp}}$ gauge charge (Q^{sp}) and $U(1)_{\text{ch}}$ gauge charge (Q^{ch}). Here the $U(1)_{\text{sp}}$ gauge charge is defined on the

TABLE I. Different kinds of gauge charges carried by various excitations. Q^{em} , Q^{sp} , and Q^{ch} refer to the electric charge, $U(1)_{\text{sp}}$ gauge charge, and $U(1)_{\text{ch}}$ gauge charge, respectively. q_e is the charge of the electron.

Operator	Q^{em}	Q^{sp}	Q^{ch}
$c_{i\sigma}^\dagger$	q_e	0	0
$f_{i\sigma}^\dagger$	0	1	0
$e^{i\theta_i}$	q_e	-1	0
$\Phi_{\mathbf{r}}^\dagger, \mathbf{r} \in A$	$q_e/2$	-1/2	1
$\Phi_{\mathbf{r}}^\dagger, \mathbf{r} \in B$	$-q_e/2$	1/2	1

pyrochlore lattice site as $Q_i^{\text{sp}} = \sum_{\sigma} f_{i\sigma}^\dagger f_{i\sigma} - L_i^z$ and the local $U(1)_{\text{ch}}$ gauge charge is defined on the dual diamond lattice site [see Fig. 1(c)] as $Q_{\mathbf{r}}^{\text{ch}} = \eta_{\mathbf{r}} \sum_{\mu} L_{\mathbf{r}, \mathbf{r} + \eta_{\mathbf{r}} \mathbf{e}_{\mu}}^z$ where $\eta_{\mathbf{r}} = +1(-1)$ for \mathbf{r} on the A(B) sublattice of the dual diamond lattice and \mathbf{e}_{μ} are the four nearest-neighbor vectors from the A sublattice sites [see Fig. 1(c)]. The charge- $q_e/2$ bosons are fully gapped in the Mott insulator. As the electron hopping t increases, the charge excitation gap becomes smaller and the charged bosons condense upon closing the gap. The condensation of charge- $q_e/2$ bosons would make the two internal gauge fields [$U(1)_{\text{sp}}$ and $U(1)_{\text{ch}}$] massive simultaneously, and drives a phase transition to a Fermi liquid metal [see Fig. 1(e)]. Therefore, there are only two phases in the phase diagram [see Fig. 1(e)], which is consistent with the quantum Monte Carlo simulation results for an interacting hardcore boson model at the half-filling on the pyrochlore lattice [28].

In order to clearly represent both the $U(1)_{\text{ch}}$ gauge structure and charge fractionalization, and to study the boson condensation transition for the charge sector H_{ch} , we employ the parton-gauge construction that was recently applied to the quantum spin ice [27,29–31]. We include both the fractionalized charge bosons and a gauge field in the rotor variable as $e^{i\theta_i} = \Phi_{\mathbf{r}}^\dagger \Phi_{\mathbf{r}'} l_{\mathbf{r}\mathbf{r}'}^+$, $L_i^z = l_{\mathbf{r}\mathbf{r}'}^z$, where the pyrochlore lattice site $i = \mathbf{r} + (\mathbf{e}_{\mu}/2)$ is the midpoint of the link ($\mathbf{r}\mathbf{r}'$) on the dual diamond lattice and $\mathbf{r}(\mathbf{r}' = \mathbf{r} + \mathbf{e}_{\mu})$ belongs to the A(B) diamond sublattice. Here, $l_{\mathbf{r}\mathbf{r}'}^z \equiv E_{\mathbf{r}\mathbf{r}'}$ and $l_{\mathbf{r}\mathbf{r}'}^{\pm} \equiv \Delta_{\mathbf{r}\mathbf{r}'} e^{\pm i A_{\mathbf{r}\mathbf{r}'}}$ ($\Delta_{\mathbf{r}\mathbf{r}'} \equiv |l_{\mathbf{r}\mathbf{r}'}^{\pm}|$) represent the lattice $U(1)_{\text{ch}}$ gauge fields on the links of the dual diamond lattice. To constrain the enlarged Hilbert space, we need $[\Phi_{\mathbf{r}}, Q_{\mathbf{r}}^{\text{ch}}] = \Phi_{\mathbf{r}}$ and $[\Phi_{\mathbf{r}}^\dagger, Q_{\mathbf{r}}^{\text{ch}}] = -\Phi_{\mathbf{r}}^\dagger$. Now it is clear that the electron in the CMI fractionalizes into two charge- $q_e/2$ bosons and a fermionic spinon [with an open string operator $l_{\mathbf{r}, \mathbf{r} + \mathbf{e}_{\mu}}^+$ connecting two bosons; see Fig. 1(d)],

$$c_{\mathbf{r} + \frac{\mathbf{e}_{\mu}}{2}, \sigma}^\dagger = f_{\mathbf{r} + \frac{\mathbf{e}_{\mu}}{2}, \sigma}^\dagger \Phi_{\mathbf{r}}^\dagger \Phi_{\mathbf{r} + \mathbf{e}_{\mu}} l_{\mathbf{r}, \mathbf{r} + \mathbf{e}_{\mu}}^+, \quad (5)$$

where $\mathbf{r} \in A$ sublattice. With the above construction, the charge sector Hamiltonian can be written as

$$H_{\text{ch}} = -J^{\text{eff}} \sum_{\mathbf{r}, \mu \neq \nu} \Phi_{\mathbf{r}+\eta_{\mu}\mathbf{e}_{\mu}}^{\dagger} \Phi_{\mathbf{r}+\eta_{\nu}\mathbf{e}_{\nu}} \Gamma_{\mathbf{r}, \mathbf{r}+\eta_{\mu}\mathbf{e}_{\mu}}^{-\eta_{\mu}} \Gamma_{\mathbf{r}, \mathbf{r}+\eta_{\nu}\mathbf{e}_{\nu}}^{+\eta_{\nu}} + \frac{V}{2} \sum_{\mathbf{r}} (Q_{\mathbf{r}}^{\text{ch}})^2, \quad (6)$$

where we have dropped the linear L^z term because of the emergent particle-hole symmetry at the Mott transition. The above charge Hamiltonian describes the minimal coupling of the fractionally charged bosons with the emergent $U(1)_{\text{ch}}$ gauge field on the dual diamond lattice. Within the gauge mean-field approximation [27], we show that the Mott transition occurs at $(V/J^{\text{eff}})_c \approx 5.21$, where the charge bosons develop an energy gap. In this calculation, we have treated L^z and l^z as spin- $\frac{1}{2}$ variables, which is a good approximation since double occupancy (or $L^z = \frac{3}{2}$) configuration is strongly suppressed by the large on-site interaction U . Together with the self-consistent mean-field theory for H_{sp} , we obtain a continuous Mott transition at $(V/t)_c \approx 1.65$ [see Fig. 1(e)].

Weak Mott regime for $\frac{1}{8}$ filling. For the CMI with $\frac{1}{8}$ electron filling, the main difference is that the electron occupation number per tetrahedron is 1, i.e., $\sum_{i \in \text{tet}} L_i^z = -1$. The low energy model of the charge sector is then obtained through the ring hopping processes of the rotors around a hexagon [see Fig. 1(b)]. In the end, the charge occupation-number constraint and the low energy model are identical to the $\frac{1}{2}$ -magnetization plateau state of a spin- $\frac{1}{2}$ XXZ model on the pyrochlore lattice in a uniform magnetic field [20]. It is known that the $\frac{1}{2}$ -magnetization plateau state is a $U(1)$ QSL with the same universal properties as the quantum spin ice [20]. Therefore, the charge sector for the $\frac{1}{8}$ -filled case is also a $U(1)_{\text{ch}}$ FCL with the same low energy excitations as the $\frac{1}{4}$ -filled case.

Strong Mott regime. Here we turn to the strong Mott regime with $V \gg t$. Let us start with the CMI at the $\frac{1}{8}$ -filling, where the electrons on neighboring tetrahedra are always separated by one unoccupied site [see Fig. 1(b)]. The dominant interaction arises from the ring hopping processes of the three electrons on the hexagon and is described by

$$H_{\text{eff}} = -J_{\text{ring}}^e \sum_{\text{hexagon}} \sum_{\alpha\beta\gamma} (c_{1\alpha}^{\dagger} c_{2\alpha} c_{3\beta}^{\dagger} c_{4\beta} c_{5\gamma}^{\dagger} c_{6\gamma} + c_{1\alpha}^{\dagger} c_{6\alpha} c_{5\beta}^{\dagger} c_{4\beta} c_{3\gamma}^{\dagger} c_{2\gamma} + \text{H.c.}), \quad (7)$$

where $J_{\text{ring}}^e = (6t^3/V^2)$ is the electron ring hopping amplitude. This interaction does not transfer charges between tetrahedra, but does transfer spin quantum numbers and hence overwhelms any other spin-spin interactions that arise from higher order processes. We emphasize that Eq. (7) *cannot* be cast into the usual form of pairwise spin interactions or ring exchange, which is an important difference between the CMIs and conventional magnets.

In conventional magnets, the spin moment can be considered as being coupled to a mean magnetic field generated by the exchange interactions from neighboring spins and if this mean magnetic field does not fluctuate strongly, the spin tends to align with this field and develop magnetic ordering. For the CMI here, such a mean magnetic field cannot be defined from the interaction in Eq. (7) and thus we do not expect simple magnetic ordering. Then, for the spin sector, we may expect the QSL from the weak Mott regime to remain in the strong Mott regime. For the charge sector, we note that the effect of Eq. (7) on the charge excitations is identical to the charge rotor hopping processes in Eq. (4). Following the same reasoning as presented for the weak Mott regime, we expect the same $U(1)_{\text{ch}}$ FCL to arise in the strong Mott regime. In other words, the quasi-itinerancy nature of the electrons inside the FCL helps the spin quantum numbers to freely propagate, which prevents simple magnetic ordering and may stabilize a QSL state. This quasi-itinerancy would be a new mechanism to stabilize quantum spin liquid phases, in addition to the known mechanisms such as geometric frustration, low-dimensionality, and the proximity to Mott transitions.

In the strong Mott regime for the $\frac{1}{4}$ -filling, there exists a superexchange spin-spin interaction between nearest neighbor sites with the exchange coupling $J_{\text{ex}} = 4t^2/(U - V) + 8t^3/V^2$. Since this energy scale J_{ex} is larger than or comparable to the electron ring hopping amplitude J_{ring}^e , the FCL/QSL may survive or be destabilized depending on different parameter regimes [32].

Discussion. We now discuss the experimental signatures related to these exotic CMIs. We begin with the principal physical properties in the vicinity of the Mott transition. The Mott transition is continuous in the mean-field theory, but might turn to a weakly first order transition upon including $U(1)_{\text{ch}}$ gauge fluctuations [33]. Even in that case, the first-order effect may be important only at extremely low temperatures. So for a rather wide temperature range, the physics near the Mott transition is controlled by the *critical* fractionalized charge bosons coupled to the $U(1)_{\text{ch}}$ and $U(1)_{\text{sp}}$ gauge fields, and the fermionic spinons coupled to the $U(1)_{\text{sp}}$ gauge field. Similarly to the half-filled case studied earlier [7], the dynamical critical exponent for the charge boson [fermionic spinon with $U(1)_{\text{sp}}$] is $z = 1$ ($z = 3$). Hence we expect two crossover temperature scales for specific heat and electric resistivity, respectively. Due to further fractionalization of charge excitations, the tunneling density of states at the transition would be highly suppressed as $N_{\text{tunn}}^{\text{crit}}(\omega) \sim \omega^4$ instead of ω^2 as in the half-filled case [7].

The low energy $U(1)_{\text{ch}}$ gauge field originates from the electron charge fluctuations and may be probed by elastic and/or inelastic x-ray scattering. Similarly to the spin structure factor in the quantum spin ice [26–28,34], the inelastic charge structure factor of the CMI at low energies can be regarded as the emergent “electric-field”

correlator and is given by $\text{Im}[E_{-\mathbf{k},-\omega}^\alpha E_{\mathbf{k},\omega}^\beta] \propto [\delta_{\alpha\beta} - (k_\alpha k_\beta / \mathbf{k}^2)] \omega \delta(\omega - v|\mathbf{k}|)$, where $\mathbf{E}_{\mathbf{r}+\frac{1}{2}\mathbf{e}_\mu} \equiv L_{\mathbf{r},\mathbf{r}+\mathbf{e}_\mu}^z(\mathbf{e}_\mu/|\mathbf{e}_\mu|) = (n_{\mathbf{r}+\frac{1}{2}\mathbf{e}_\mu} - \frac{1}{2})(\mathbf{e}_\mu/|\mathbf{e}_\mu|)$ and $\mathbf{r} \in A$ diamond sublattice. Here v is the speed of the $U(1)_{\text{ch}}$ gauge photon.

The CMI is expected to lose the quantum coherence around a temperature $T^* \sim \max[J_{\text{ring}}^e, J^{\text{ex}}]$ in the Mott regime. In the temperature range $T^* \lesssim T \lesssim V$, the cluster electron occupation-number constraint still holds and the system is described by a thermal charge liquid, where degenerate charge configurations are equally allowed. Similarly to the classical spin ice [19], the equal-time charge structure factor is given by $\langle E_{-\mathbf{k}}^\alpha E_{\mathbf{k}}^\beta \rangle \propto \delta_{\alpha\beta} - (k_\alpha k_\beta / \mathbf{k}^2)$, which leads to the pinch point structures in the \mathbf{k} space [19,23–25].

There exist several candidate materials for $\frac{1}{4}$ or $\frac{1}{8}$ -filled pyrochlore lattice systems. Various spinels such as LiV_2O_4 (with $\text{V}^{3.5+}:d^{1.5}$) [14], CuIr_2S_4 (with $\text{Ir}^{3.5+}:d^{5.5}$) [17] and GaTa_4Se_8 (with $\text{Ta}^{3.25+}:d^{1.75}$) [15] may be good candidates for $\frac{1}{4}$ and $\frac{1}{8}$ -filling cases. The β -pyrochlore system CsW_2O_6 (with $\text{W}^{5.5+}:d^{0.5}$) [16] may also be a promising system where the physics discussed here can be explored.

This work was supported by the NSERC, CIFAR, and Centre for Quantum Materials at the University of Toronto. G. C. thanks Q. Si for the hospitality during his visit to Rice University when a related idea was motivated. Y. B. K. thanks S. Isakov for an earlier collaboration in related ideas. We also thank J.-H. Jiang, A. Burkov, and A. Paramekanti for illuminating discussions.

[1] M. Imada, A. Fujimori, and Y. Tokura, *Rev. Mod. Phys.* **70**, 1039 (1998).
 [2] O. I. Motrunich, *Phys. Rev. B* **72**, 045105 (2005).
 [3] S.-S. Lee and P. A. Lee, *Phys. Rev. Lett.* **95**, 036403 (2005).
 [4] L. Balents, *Nature (London)* **464**, 199 (2010).
 [5] T. Senthil, *Phys. Rev. B* **78**, 045109 (2008).
 [6] T. Senthil, *Phys. Rev. B* **78**, 035103 (2008).
 [7] D. Podolsky, A. Paramekanti, Y. B. Kim, and T. Senthil, *Phys. Rev. Lett.* **102**, 186401 (2009).
 [8] Y. Shimizu, K. Miyagawa, K. Kanoda, M. Maesato, and G. Saito, *Phys. Rev. Lett.* **91**, 107001 (2003).
 [9] Y. Okamoto, M. Nohara, H. Aruga-Katori, and H. Takagi, *Phys. Rev. Lett.* **99**, 137207 (2007).
 [10] G. Chen and Y. B. Kim, *Phys. Rev. B* **87**, 165120 (2013).
 [11] J. P. Sheckelton, J. R. Neilson, D. G. Soltan, and T. M. McQueen, *Nat. Mater.* **11**, 493 (2012); J. P. Sheckelton, F. R. Foronda, L. D. Pan, C. Moir, R. D. McDonald, T. Lancaster, P. J. Baker, N. P. Armitage, T. Imai, S. J. Blundell, and T. M. McQueen, *Phys. Rev. B* **89**, 064407 (2014); M. Mourigal, W. T. Fuhrman, J. P. Sheckelton,

A. Wattle, J. A. Rodriguez-Rivera, D. L. Abernathy, T. M. McQueen, and C. L. Broholm, *Phys. Rev. Lett.* **112**, 027202 (2014).
 [12] G. Chen, H. Y. Kee, and Y. B. Kim, [arXiv:1408.1963](https://arxiv.org/abs/1408.1963).
 [13] P. Fulde, K. Penc, and N. Shannon, *Ann. Phys. (Amsterdam)* **11**, 892 (2002).
 [14] C. Urano, M. Nohara, S. Kondo, F. Sakai, H. Takagi, T. Shiraki, and T. Okubo, *Phys. Rev. Lett.* **85**, 1052 (2000).
 [15] M. M. Abd-Elmeguid, B. Ni, D. I. Khomskii, R. Pocha, D. Johrendt, X. Wang, and K. Syassen, *Phys. Rev. Lett.* **93**, 126403 (2004).
 [16] D. Hirai, M. Bremholm, J. M. Allred, J. Krizan, L. M. Schoop, Q. Huang, J. Tao, and R. J. Cava, *Phys. Rev. Lett.* **110**, 166402 (2013).
 [17] P. G. Radaelli, Y. Horibe, M. J. Gutmann, H. Ishibashi, C. H. Chen, R. M. Ibberson, Y. Koyama, Y. S. Hor, V. Kiryukhin, and S. W. Cheong, *Nature (London)* **416**, 155 (2002).
 [18] E. Runge and P. Fulde, *Phys. Rev. B* **70**, 245113 (2004).
 [19] C. Henley, *Annu. Rev. Condens. Matter Phys.* **1**, 179 (2010), and references therein.
 [20] D. L. Bergman, G. A. Fiete, and L. Balents, *Phys. Rev. B* **73**, 134402 (2006).
 [21] For the uniform nearest-neighbor hopping model, the Fermi level lies at a flat band extending from X to W in the Brillouin zone for the $1/4$ -filling case. In principle, this flat Fermi surface may cause other instabilities. For a generic tight-binding model (for example, with a spin-dependent hopping amplitude), such a flat band and instabilities may be avoided.
 [22] S. Florens and A. Georges, *Phys. Rev. B* **70**, 035114 (2004).
 [23] S. T. Bramwell and M. J. P. Gingras, *Science* **294**, 1495 (2001).
 [24] C. Castelnovo, R. Moessner, and S. L. Sondhi, *Nature (London)* **451**, 42 (2008).
 [25] M. Gingras, *Science* **326**, 375 (2009).
 [26] M. Hermele, M. P. A. Fisher, and L. Balents, *Phys. Rev. B* **69**, 064404 (2004).
 [27] L. Savary and L. Balents, *Phys. Rev. Lett.* **108**, 037202 (2012).
 [28] A. Banerjee, S. V. Isakov, K. Damle, and Y. B. Kim, *Phys. Rev. Lett.* **100**, 047208 (2008).
 [29] L. Savary and L. Balents, *Phys. Rev. B* **87**, 205130 (2013).
 [30] Y.-P. Huang, G. Chen, and M. Hermele, *Phys. Rev. Lett.* **112**, 167203 (2014).
 [31] S. B. Lee, S. Onoda, and L. Balents, *Phys. Rev. B* **86**, 104412 (2012).
 [32] G. Chen, H. Y. Kee, and Y. B. Kim (unpublished).
 [33] B. I. Halperin, T. C. Lubensky, and S. k. Ma, *Phys. Rev. Lett.* **32**, 292 (1974).
 [34] N. Shannon, O. Sikora, F. Pollmann, K. Penc, and P. Fulde, *Phys. Rev. Lett.* **108**, 067204 (2012); O. Sikora, F. Pollmann, N. Shannon, K. Penc, and P. Fulde, *Phys. Rev. Lett.* **103**, 247001 (2009); O. Benton, O. Sikora, and N. Shannon, *Phys. Rev. B* **86**, 075154 (2012).